VOLUME 35 NUMBER 1

ACCOUNTS of CHEMICAL RESEARCH®

JANUARY 2002

Identifying Hydrogen Bond Alignments in Multistranded DNA Architectures by NMR

ANANYA MAJUMDAR* AND DINSHAW J. PATEL

Cellular Biochemistry and Biophysics Department, Memorial Sloan-Kettering Cancer Center, 1275 York Avenue, New York, New York 10021

Received June 26, 2001

ABSTRACT

NMR studies of nucleic acids have benefited tremendously from the discovery of trans-hydrogen-bond scalar coupling constants, which have enabled direct determination of N−H···N and N−H···O=C hydrogen bonds using a combination of $^{2h}J_{NN}$-, $^{4h}J_{NN}$-, and $^{3h}J_{NC}$-based spectroscopy. This is especially true of multistranded DNA architectures containing intricate hydrogen-bonded networks mediated primarily through mismatched base pairing, which often resist identification by posing serious technical, spectroscopic, and physicochemical challenges. In this Account, we present a suite of NMR pulse sequences that have been developed in our laboratory to address these issues. We demonstrate the utility of these methods for identifying hydrogen bonds in two quadruplex DNA structures, containing triad, tetrad, and hexad motifs involving Watson−Crick, G·G and sheared G·A mismatch base pairing.

Introduction

The polymorphic nature of DNA[1] manifests itself in a variety of multistranded architectures that depart from canonical *B*-DNA structures, mostly in purine-rich sequences. These include triplexes, quadruplexes and junctions, parallel DNA, and i-motifs, exhibiting a wide range of strand directionalities and mismatch base-pairing alignments (reviewed in ref 2). Such architectures, especially quadruplexes, have been implicated in various biological processes involving telomere and centromere function[2,3−6] replication, transcription, and recombination,[7] and in triplet-repeat disease sequences,[2] thereby providing new insights into nucleic acid structure−function relationships, and carrying potential applications in therapeutics. In our laboratory, considerable effort has gone into identifying such higher order DNA structures in purine-rich sequences.[2]

The global folds and topologies of higher-order nucleic acid structures are dictated to a large extent by an intricate network of hydrogen bonds, resulting in the formation of diverse structural elements or motifs. Unambiguous identification of these hydrogen-bonded networks is, therefore, a critical component in the structure determination of multistranded DNA. Conventional NMR spectroscopy has relied heavily on indirect lines of evidence derived from properties of hydrogen-bonded protons, such as changes in chemical shifts, chemical exchange rates, and NOEs, all of which are susceptible to errors in interpretation. Recently, this scenario was dramatically altered by a landmark discovery—made nearly simultaneously by the groups of Grzesiek[8] and Wüthrich[9]—wherein it was showed that in ^{15}N-labeled nucleic acids, an N_d−H···N_a hydrogen

* To whom correspondence should be addressed. Phone: (212) 639-2791. Fax: (212) 717-3453. E-mail: majumdar@sbnmr1.mskcc.org.

Ananya Majumdar was born in Delhi, India. He obtained his B.S. in chemistry from the University of Delhi (1984), Masters in chemistry from the Indian Institute of Technology, Kanpur, India (1986), and Ph.D. in physical chemistry from the Tata Institute of Fundamental Research (TIFR), Mumbai, India (1991). After a postdoctoral fellowship at the University of Michigan (1992−1994), he spent three years as a Fellow at TIFR, Mumbai, 1994−1997, after which he joined the Memorial Sloan-Kettering Cancer, New York, as a Research Associate. He is presently Assistant Laboratory Member. His research interests lie primarily in biomolecular NMR methodology development.

Dinshaw J. Patel is a native of Mumbai, India. He received his B.S. in chemistry from the University of Bombay and his Ph.D. in chemistry in 1968 from New York University. After postdoctoral training at NYU Medical School and Bell Laboratories, he spent 15 years as a Member of the Technical Staff in the Polymer Chemistry department of Bell Labs, followed by 8 years as a Professor, Department of Biochemistry and Molecular Biophysics, at the College of Physicians and Surgeons, Columbia University. He started his current appointment in 1992 as Member in the Cellular Biochemistry and Biophysics Program of the Memorial Sloan-Kettering Cancer Center. Dr. Patel's research focuses on the application of NMR techniques to nucleic acid structure, dynamics, and recognition, including studies of multistranded DNA architectures, carcinogenic damage sites and antitumor drug complexes, adaptive conformational transitions of RNAs bound to cofactors, peptides, and saccharides, with emphasis on structure−function relationships. He received the Distinguished Technical Staff Award of Bell Labs in 1983, the Distinguished Alumnus Award of NYU in 1997, has served on the Scientific and Medical Advisory Boards of the Howard Hughes Medical Institute, is a past-president of the Harvey Society, and is the current incumbent of the Abby Rockefeller Mauze Chair in Experimental Therapeutics at Sloan-Kettering.

10.1021/ar010097+ CCC: $22.00
Published on Web 12/21/2001

bond is characterized by a scalar coupling constant ($^{2h}J_{NdNa}$) between the donor (N_d) and acceptor nitrogens (N_a). Although scalar couplings across hydrogen bonds had been observed previously in proteins in other contexts[10,11] and other molecules,[12] this discovery was the first of its kind in nucleic acids. Subsequently, several other such trans-hydrogen bond couplings have been discovered (see refs 13−16 and references therein); those relevant for nucleic acids being the one-bond $^{1h}J_{HNa}$ couplings across $N_d-H\cdots N_a$ bonds,[9,17] $^{4h}J_{NdNa}$ couplings across $N_d-H\cdots O{=}C-N_a$ bonds,[18] and $^{3h}J_{NC'}$ couplings between the donor nitrogen and acceptor carbonyl carbon across $N_d-H\cdots O{=}C'$ hydrogen bonds[19] in $^{15}N/^{13}C$-labeled nucleic acids. Intermolecular trans-hydrogen bond couplings have also been reported, such as $^{2h}J_{NN}$ couplings across N−H···N hydrogen bonds between arginine side chains and guanine bases in peptide−RNA complexes[20] and $^{3h}J_{NP}/^{2h}J_{HP}$ couplings across N−H···O−P hydrogen bonds between phosphate and amide groups in nucleotide−protein complexes.[21,22] By providing direct evidence for the presence of hydrogen bonds in nucleic acids and their complexes, these discoveries have tremendously impacted NMR studies of nucleic acids. The $^{2h}J_{NN}$ scalar couplings are the largest (2−11 Hz) and, therefore, most easily detected by modern NMR techniques. The $^{1h}J_{HN}$ (<4 Hz), $^{4h}J_{NN}$, and $^{3h}J_{NC'}$ couplings (<0.2 Hz) are considerably smaller, and therefore, $^{2h}J_{NN}$-correlated spectroscopy has become the method of choice for exploring hydrogen-bonded networks in nucleic acids.

Since the discovery of trans-hydrogen-bond coupling constants, a number of successful applications to nucleic acid structure and dynamics have appeared in the literature,[17−42,47,51] including significant developments in methodology[17−22,31−42,50] and quantum-chemical calculations[12,43−46] relating these coupling constants to hydrogen bond lengths and bond angles (for comprehensive reviews, see refs 13−16). In our laboratory, we have focused primarily on the determination of novel structural motifs in multistranded DNA quadruplexes, including triads,[26] tetrads,[25,27,47] pentads,[47] and hexads.[25] In the process, a number of serious problems were encountered: inefficient NMR magnetization transfer across $N_d-H\cdots N_a$ bonds as a result of a wide separation of N_d and N_a chemical shifts and small $^{4h}J_{NN}$ coupling constants across N−H···O=C−N bonds; extinction of hydrogen-bonded proton resonances as a result of exchange broadening effects and problems associated with assignment of acceptor nitrogens (N_a) due to poor spectroscopic dispersion of these nuclei.

In this Account, we review the development of NMR methodology in our laboratory toward the study of multistranded DNA quadruplex architectures. The purpose is 2-fold: (a) to demonstrate the use of $^{2h}J_{NN}$-spectroscopy-based protocols for unambiguous identification of hydrogen bonding networks within the motifs contained in these structures and (b) to highlight the NMR methodology designed to address the above-mentioned problems that arose in the process. We use two quadruplex DNA architectures, a G·(C−A) triad containing dimer and a four-stranded, A·(G·G·G·G)·A hexad-containing tetramer, to illustrate applications as well as methodology.

Structures and Motifs. Figures 1 and 2 show two DNA systems whose structures have recently been determined in our laboratory, each possessing unique hydrogen-bonded motifs. The molecule in Figure 1a, $d(G_1G_2G_3T_4T_5C_6A_7G_8G_9)$ ("the triad system", mol wt ∼ 6 kDa),[26] is a 2-fold symmetric G quadruplex consisting of G1·G2·G8·G9 tetrads (Figure 1c) sandwiched between G3·(C6−A7) triads (Figure 1b). Figure 2a shows a four-stranded architecture $d(G_1C_2G_3G_4A_5G_6G_7A_8T_9)$ ("the hexad system", mol wt ∼ 11 kDa) consisting of stacked G4·G7·G4·G7 tetrads (Figure 2b), G1·C2·G1·C2 tetrads (Figure 2c), and a novel motif, the A5·(G3·G6·G3·G6)·A5 hexad[25] (Figure 2d). It is clear that the structural motifs in these systems are held together primarily by G·G and sheared G·A mismatch alignments via $N-H_2\cdots N$-type hydrogen bonds involving amino protons. Three distinct categories of hydrogen bonds are recognized: (a) Watson−Crick (G)-N1H1···N3(C), (b) (A)N6H_2···N3(G), and (c) (A/G)NH_2···N7(A/G). We use these two systems to illustrate the experimental protocols that were developed to identify these hydrogen bonds in $^{13}C/^{15}N$-labeled samples[48] in order to reveal the relevant structural motifs. Detailed descriptions of all NMR methodology described here may be found in refs 8, 18, 31, 33, 37, and 50. Conceptual aspects of $^{2h}J_{NN}$ spectroscopy are discussed in detail in the review by Dingley et al.[13]

The Triad System. The key motif in this system is the G3·(C6-A7) triad,[28] consisting of Watson−Crick pairing between G3 and C6, and sheared G3·A7 mismatch alignment between G3 and A7 via (A7)N6H_2···G3(N3) and (G3)N2H_2···N7(A7) hydrogen bonds (Figure 1b). The G1·G2·G8·G9 tetrad is composed of Watson−Crick to Hoogsteen edge alignments between adjacent guanines, involving (G*p*)N2H_2···N7(G*q*) hydrogen bonds (Figure 1c).

HNN-COSY. The Watson−Crick G3·C6 base pair in the triad is easily identified from an HNN-COSY spectrum (Figure 3a) in which NMR magnetization transfer takes place as follows: H1(G)→N1(G)→N3(C,t_1)→N1→H1(t_2). In the final spectrum, the H1 (imino) proton of G3 shows two correlations: an auto peak to the directly bonded, donor N1 nitrogen of G3 and a cross peak (of opposite sign) to the acceptor N3 nitrogen of C6, mediated by the $^{2h}J_{N1N3}$ coupling between N1(G3) and N3(C6). The imino protons of the guanine bases belonging to the G1·G2·G8·G9 tetrad (Figure 1c) do not exhibit similar cross peaks, because they are hydrogen bonded to C=O groups rather than to nitrogen.

HN(N)-TOCSY and H(N)CO-(NN)-TOCSY. To identify the $N1_p-H1_p\cdots O{=}C6_q-N1_q$ connectivities within the G1·G2·G8·G9 tetrad, we developed pulse sequences based on magnetization transfer between the $N1_p$ and $N1_q$ nitrogens via the small (<0.15 Hz), four-bond $^{4h}J_{NpNq}$ coupling.[18] These experiments, based on efficient $^{15}N-^{15}N$ magnetization transfer via band-selective isotropic mixing,[53,54] are suitable for correlating ^{15}N nuclei, which are very close in frequency and correlated via small couplings. The HN-(N)-TOCSY experiment[18] yields correlations between ($N1_p$)-

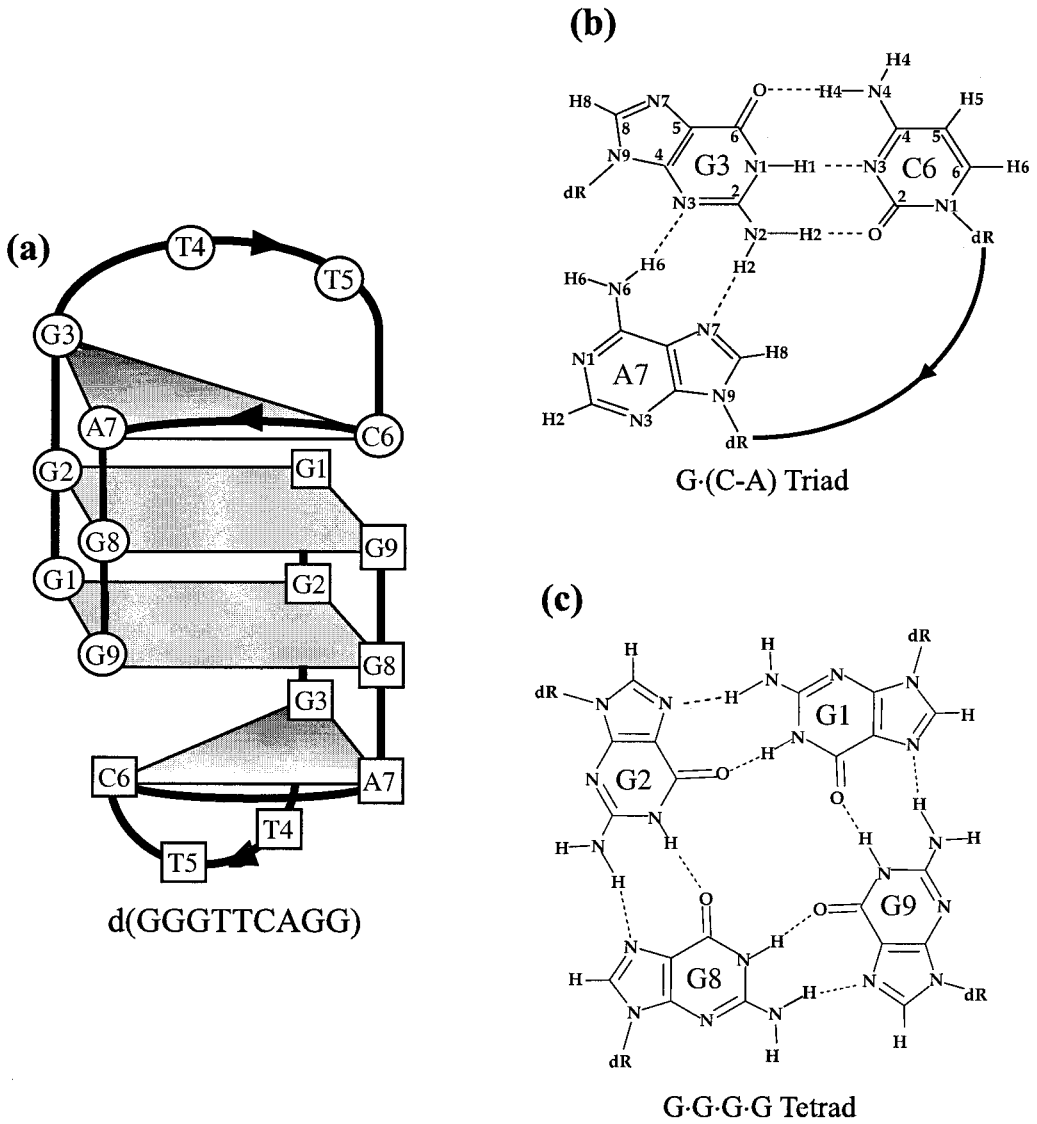

FIGURE 1. (a) Schematic representation of the dimeric DNA quadruplex d(GGGTTCAGG),[26] (b) the G3·(C6−A7) triad consisting of Watson−Crick G3−C6 and sheared G3·A7 alignments, and (c) the G1·G2·G8·G9 tetrad composed of Watson−Crick to Hoogsteen edge alignments of adjacent guanines.

$H1_p$ protons and $N1_q$ nitrogens, but the complementary CP-H(N)CO-(NN)-TOCSY experiment[18] includes additional band-selective $^{15}N-^{13}C$ cross-polarization periods to yield correlations between $(N1_p)H1_p$ protons and $C6_q$ carbons. The HN(N)-TOCSY and CP-H(N)CO-(NN)-TOCSY spectra of the triad system are shown in Figure 3b, and 3c, respectively, demonstrating auto and sequential connectivities between imino protons and trans-hydrogen-bond nitrogens (Figure 3b) and carbons (Figure 3c) within the G1·G2·G8·G9 tetrad. Note that the degeneracy of the N1 chemical shifts of G8 and G9, which prevents identification of the G8:G9 connectivity from the HN(N)-TOCSY spectrum, is lifted in the CP-H(N)CO-(NN)-TOCSY spectrum, which clearly establishes this linkage. On the other hand, the G2:G8 correlation, which is easily observable in the HN(N)-TOCSY spectrum, is not observable in the CP-H(N)CO-(NN)-TOCSY spectrum, owing to degeneracy of the C6 carbons of G2 and G8. Clearly, the two experiments bear a complementary relationship. Recently, Dingley et al.[19] obtained correlations between $(N1_p)$ $H1_p$ protons and $C6_q$ carbons via $^{3h}J_{NpCq}$ couplings (<0.2 Hz) between $N1_p$ nitrogens and $C6_q$ carbons using long-range HNCO experiments. As a result of the rather small value of the $^{4h}J_{NpNq}$ and $^{3h}J_{NpCq}$ coupling constants, the success of these experiments is likely to be restricted to medium-sized molecules (<10 kD) using present day technology. In addition, these experiments require doubly ($^{15}N/^{13}C$)-labeled samples, whereas the HNN-COSY and soft-HNN-COSY (see below) sequences require only ^{15}N-labeled samples.

Soft HNN-COSY. The remaining hydrogen bonds in the triad system consist of mismatch alignments involving NH_2 protons in the (A7)$N6H_2$···G3(N3) and (G3)$N2H_2$··· N7(A7) hydrogen bonds within the sheared G3·A7 mismatch in the triad and the (G*p*)$N2H_2$···N7(G*q*) alignments within the tetrad. The (A7)$N6H_2$···G3(N3) hydrogen bond is easily obtained from an HNN-COSY spectrum (Figure 4a) in which two pairs of correlations are observed: the intraresidue $N2H_2$(G3,ω_2):N3(G3,ω_1) cross peaks and the trans-hydrogen bond $N6H_2$(A7,ω_2):N3(G3,ω_1) cross peaks

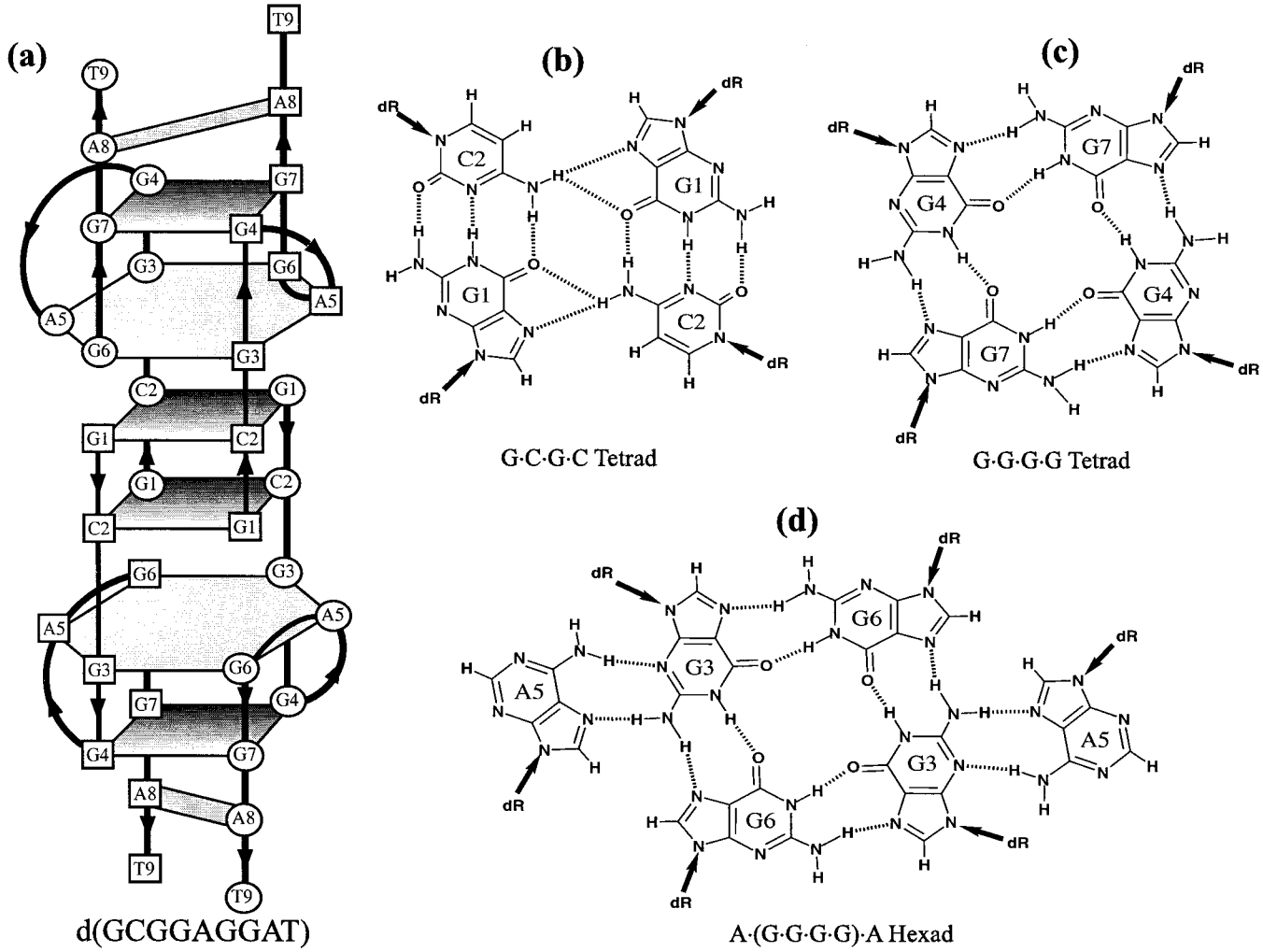

FIGURE 2. (a) Schematic representation of the tetrameric DNA quadruplex d(GCGGAGGAT), (b) the G1·C2·G1·C2 tetrad composed of dimerization of Watson−Crick G1−C2 pairs along their major groove edges, (c) the G4·G7·G4·G7 tetrad, and (d) the A5·(G3·G6·G3·G6)·A5 hexad composed of a G3·G6·G3·G6 tetrad core and a sheared G3·A5 mismatch.

mediated via the $^{2h}J_{N6N3}$ coupling (∼4 Hz). However, observation of the $^{2h}J_{N2N7}$-mediated $N2H_2(G3,\omega_2)$:N7(A7,ω_1) cross peak in the triad and the $N2H_2(Gp,\omega_2)$:N7(Gq,ω_1) cross peaks in the G1·G2·G8·G9 tetrad proved to be nearly impossible using a straightforward application of the HNN-COSY experiment because of technical difficulties in achieving efficient magnetization transfer between the amino and N7 nitrogens, which have a large chemical shift separation (150−160 ppm). To address this issue, a new method, the soft HNN-COSY, was developed,[31] which makes use of selective ^{15}N pulses. This sequence was first applied in our laboratory for detecting NH_2:N7 cross peaks in A·A mismatches[24,31] and was subsequently improved upon by Dingley et al.[19] to allow detection of both auto- and cross peaks. In the soft HNN-COSY spectrum of the triad system recorded at 0 °C (Figure 4b), the $N2H_2(G3,\omega_2)$:N7(A7,ω_1) cross peaks are clearly seen, thereby completing the identification of the sheared G3·A7 mismatch and, consequently, the complete validation of the G·(C−A) triad.

Figure 4b shows two additional cross peaks, mediated via $^{2h}J_{N2N7}$ couplings (6−8 Hz): $N2H_2(G9,\omega_2)$:N7(G1,ω_1) and $N2H_2(G8,\omega_2)$:N7(G9,ω_1), which identify two of the four $NH_2\cdots$N7 hydrogen bonds contained within the G1·G2·G8·G9 tetrad. However, the remaining two correlations, the $N2H_2$(G1):N7(G2) and $N2H_2$(G2):N7(G8) cross peaks, are absent. This is a consequence of a common problem in nucleic acids NMR, namely, exchange broadening.

Exchange Broadening. Exchange broadening of hydrogen-bonded protons beyond detection limits represents a serious impediment to HNN-COSY-type experiments. Imino protons are exchange-broadened as a result of chemical exchange with solvent and hydrogen bond breathing motions.[35] The intrinsically slower exchanging amino protons are often broadened more severely than imino protons because of rotations about the exocyclic C−N bond on an intermediate NMR time scale, even at temperatures as low as 0 °C. This situation may be remedied by recognizing that the $^{2h}J_{NN}$ scalar coupling involves the donor and acceptor nitrogens but not the hydrogen bonded proton(s). Consequently, we have developed a series of experiments geared toward detecting $N_d-H_n\cdots N_a$ hydrogen bonds via nonexchangeable protons, an approach first used by Hennig and Geierstanger[32]

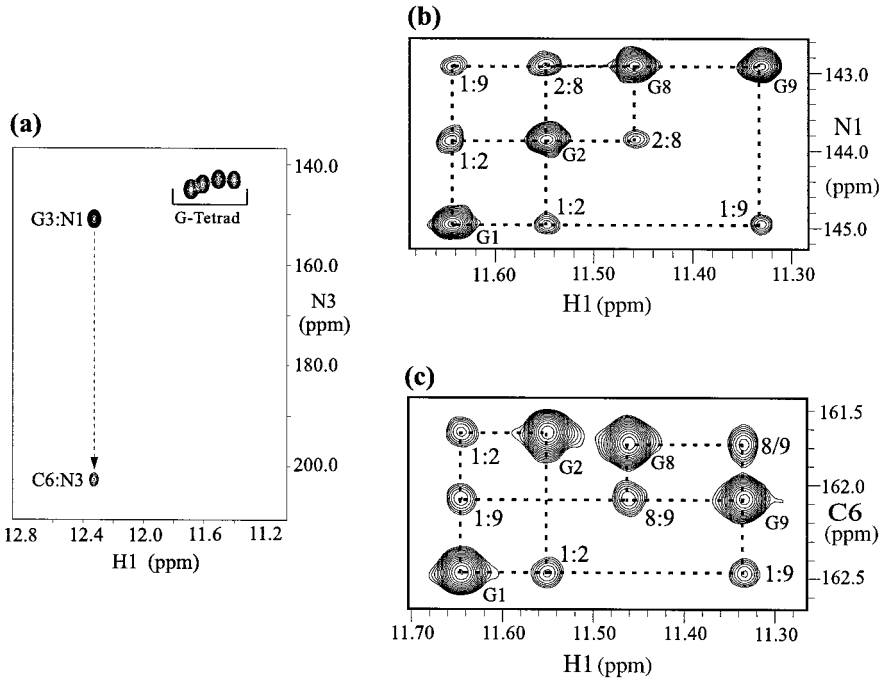

FIGURE 3. $^{2h}J_{NN}$- and $^{4h}J_{NN}$-correlated spectra to identify hydrogen bonds involving guanine imino protons in the triad and tetrad motifs within the triad system (20 °C). (a) HNN-COSY spectrum showing (G3)H1:N1(G3) auto- and $^{2h}J_{NN}$-mediated (G3)H1:N3(C6) cross peaks, establishing the G3−C6 Watson−Crick base pair within the G3·(C6-A7) triad. (b) the HN(N)-TOCSY spectrum[18] showing (G*p*)H1:N1(G*p*) auto- and (G*p*)-H1:N1(G*q*) cross peaks mediated via $^{4h}J_{NN}$ couplings, establishing the (G*p*)N_p−H···O═C_q'−N_q(G*q*) connectivities within the G1·G2·G8·G9 tetrad. The auto peaks are labeled with the identities of individual guanines, and (G*p*)H1:N1(G*q*) cross peaks are labeled p:q. (c) The CP-H(N)CO-(NN)-TOCSY spectrum[18] showing (G*p*)H1:C6(G*p*) auto- and $^{4h}J_{NN}$-mediated (G*p*)H1:C6(G*q*) cross peaks, with the same labeling scheme as in b.

in proteins. We illustrate applications of nonexchangeable $^{2h}J_{NN}$ spectroscopy to identify G·G and sheared G·A mismatches using the hexad system below as a case study.

The Hexad System. *H(CN)N(H).* From Figure 2a−d, it is evident that the hexad system consists of an intricate network of hydrogen bonds. With the exception of the G−C Watson−Crick base pair in the G1·C2·G1·C2 tetrad, all other hydrogen bonds involve amino protons. Apart from C2, all amino protons were exchange-broadened beyond detectable limits, even at 0 °C. As a result, only the G1·C2·G1·C2 tetrad could be unambiguously identified from N1H1(G1,ω_2):N3(C2,ω_1) and N4H_2(C2,ω_2):N7(G1,ω_1) cross peaks in HNN-COSY and soft HNN-COSY spectra, respectively; however, the G4·G7·G4·G7 tetrad and the A5·(G3·G6·G3·G6)·A5 hexad were completely inaccessible by these approaches. To identify these motifs, we developed the H(CN)N(H) experiment,[33] which is applicable to H−C−N_a···H_n−N_d or H−C−N_d−H_n···N_a networks, in which the nonexchangeable proton H is correlated with N_a/N_d via the magnetization transfer pathway H→$N_{a/d}$→$N_{d/a}(t_1)$→$N_{a/d}$→H(t_2) (Figure 5, lower right). The H→$N_{a/d}$ and N_a→N_d transfers are mediated via the long range $^2J_{HNa/d}$ and $^{2h}J_{NdNa}$ couplings, respectively. Trans-hydrogen-bond correlations are possible regardless of the exchange-broadened state of the hydrogen-bonded proton(s). These experiments are readily carried out in D_2O solution, since the deuterium isotope effect on the $^{2h}J_{NN}$ coupling has been determined to be only ∼0.2 Hz.[36] Moreover, depending on the stability of the hydrogen bond, experiments may be performed at higher temperatures than for HNN-COSY type of spectra, especially when amino protons are involved. Finally, by correlating a set of nuclei different from that in HNN-COSY experiments, complementary information is made available that may resolve ambiguities in HNN-COSY spectra. The H(CN)N(H) sequence was originally demonstrated on two other hexad/tetrad-containing quaduplexes[25,33] in which the key amino protons were observable, and therefore, most of the critical information was already available from soft HNN-COSY spectra. In those contexts, therefore, the H(CN)N-(H) largely played the role of augmenting the soft HNN-COSY data. For the hexad system discussed here, however, the H(CN)N(H) spectrum was the only means of identifying the G4·G7·G4·G7 tetrad and A5·(G3·G6·G3·G6)·A5 hexad units. Figure 5 shows the H8(C8N7)N(H) spectrum of the hexad system in D_2O buffer at 20 °C, from which almost all of the relevant hydrogen bonds in both the tetrads and also the hexad motif may be identified. For example, the H8(G4,ω_2):N2(G7,ω_1) and H8(G7,ω_2):N2-(G4,ω_1) cross peaks together establish the presence of the (G7)NH_2···N7(G4) and (G4)NH_2···N7(G7) hydrogen bonds, respectively, within the G4·G7·G4·G7 tetrad element. Similarly, the H8(G1,ω_2):N4(C2,ω_1) cross peak within the G1·C2·G1·C2 tetrad identifies the (C2)N4H_2···N7(G1) linkage, and the H8(G3,ω_2):N2(G6,ω_1) and H8(G6,ω_2):N2-(G3,ω_1) cross peaks identify the G3·G6·G3·G6 component of the hexad. The key signatures of hexad formation, namely, hydrogen bonds between the amino protons of G3 and the N7 nitrogens of A5 and G6, are established via the H8(A5,ω_2):N2(G3,ω_1) and H8(G6,ω_2):N2(G3,ω_1)

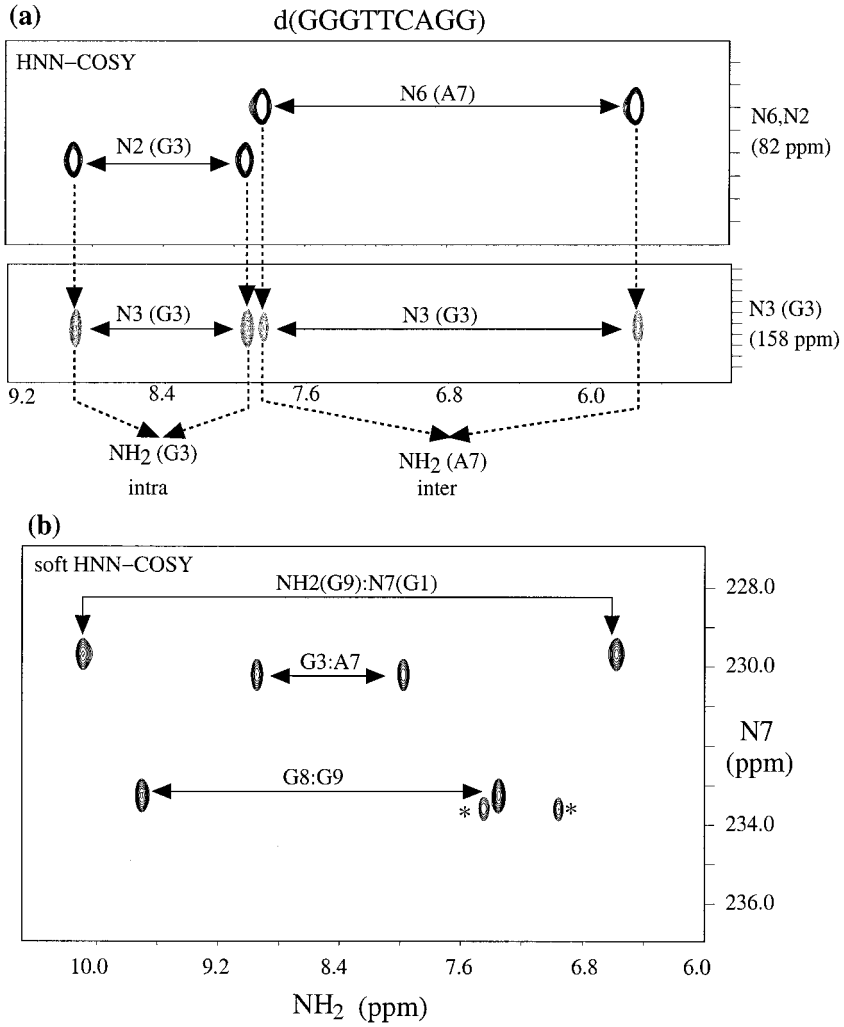

FIGURE 4. $^{2h}J_{NN}$ correlated spectra recorded on the triad system (0 °C) for identifying mismatch alignments involving amino protons in the triad and tetrad motifs (Figure 1). (a) HNN-COSY spectrum showing intranucleotide $N2H_2$(G3,ω_2):N3(G3,ω_1) (auto) and internucleotide $N6H_2$-(A7,ω_2):N3(G3,ω_1) (cross) peaks, establishing the (A7)$N6H_2$···G3(N3) hydrogen bond in the sheared G3·A7 mismatch within the triad. (b) Soft HNN-COSY spectrum showing the $N2H_2$(G3,ω_2):N7(A7,ω_1) cross peak establishing the (G3)$N2H_2$···N7(A7) linkage within the triad and $N2H_2$-(G*p*,ω_2):N7(G*q*,ω_1) cross peaks identifying two of the four (G*p*)$N2H_2$···N7(G*q*) connectivities within the tetrad. (p)NH_2···N7(q) cross peaks between nucleotides p and q are labeled p:q. The peaks marked with an asterisk (*) are folded intranucleotide $N4H_2$:N3 cross peaks from C6.

cross peaks. The relative intensities of the two cross peaks reflect differences in the respective $^{2h}J_{N2N7}$ couplings arising from differences in geometry, dynamics, or both between the G3·G6 and G3·A5 alignments.

H2N6N3 and (N)H6N6N3H2. Despite its usefulness, the H(CN)N(H) experiment does not yield one vital cross peak in the hexad system, namely, the correlation across the (A5)$N6H_2$···N3(G3) hydrogen bond. In contrast to the triad system, severe exchange-broadening of the A5 amino protons prevents the (A5)$N6H_2$:N3(G3) correlation from being observed in an HNN-COSY spectrum. Neither does the H(CN)N(H) spectrum report on this correlation, because the most suitable nonexchangeable proton, namely, H2 of A5, is situated remotely from the hydrogen bond; however, for complete validation of the hexad motif, it is critical to verify the existence of the (A5)$N6H_2$··· N3(G3) connectivity. For this purpose, we developed two experiments[37] to correlate the adenine H2 proton with the guanine N3 nitrogen via the $^{2h}J_{N6N3}$ coupling (3−4 Hz) in uniformly $^{15}N/^{13}C$-labeled samples: the "out-and-back" H2N6N3 and the "straight-through" (H6)N6N3H2 sequences. The H2N6N3 sequence follows the H2→C6→N6→N3(t_1)→N6→C6→H2(t_2) magnetization transfer pathway (Figure 6a) and is most sensitive when recorded in D_2O solution in the presence of ^2H decoupling during the N6↔N3 transfer steps. The (H6)N6N3H2 sequence, for samples in H_2O solution, is shorter and follows the H6→N6→N3(t_1)→N6→C6→H2(t_2) pathway (Figure 6b). This sequence depends critically on the efficiency of the H6→N6 step, which needs to be accomplished using spin-locking sequences to minimize exchange-broadening effects. The triad system serves as a good test system for demonstrating these techniques, since the $N6H_2$ protons of A7 (and $N2H_2$ of G3) are clearly observable, and therefore, the sheared A7·G3 mismatch is readily established using a combination of HNN-COSY (Figure 4a) and soft HNN-COSY (Figure 4b) spectra. H2N6N3 and (H6)-N6N3H2 spectra recorded on samples of the triad system in D_2O and H_2O buffer are shown in Figure 6c and d, respectively. They are identical in information content and

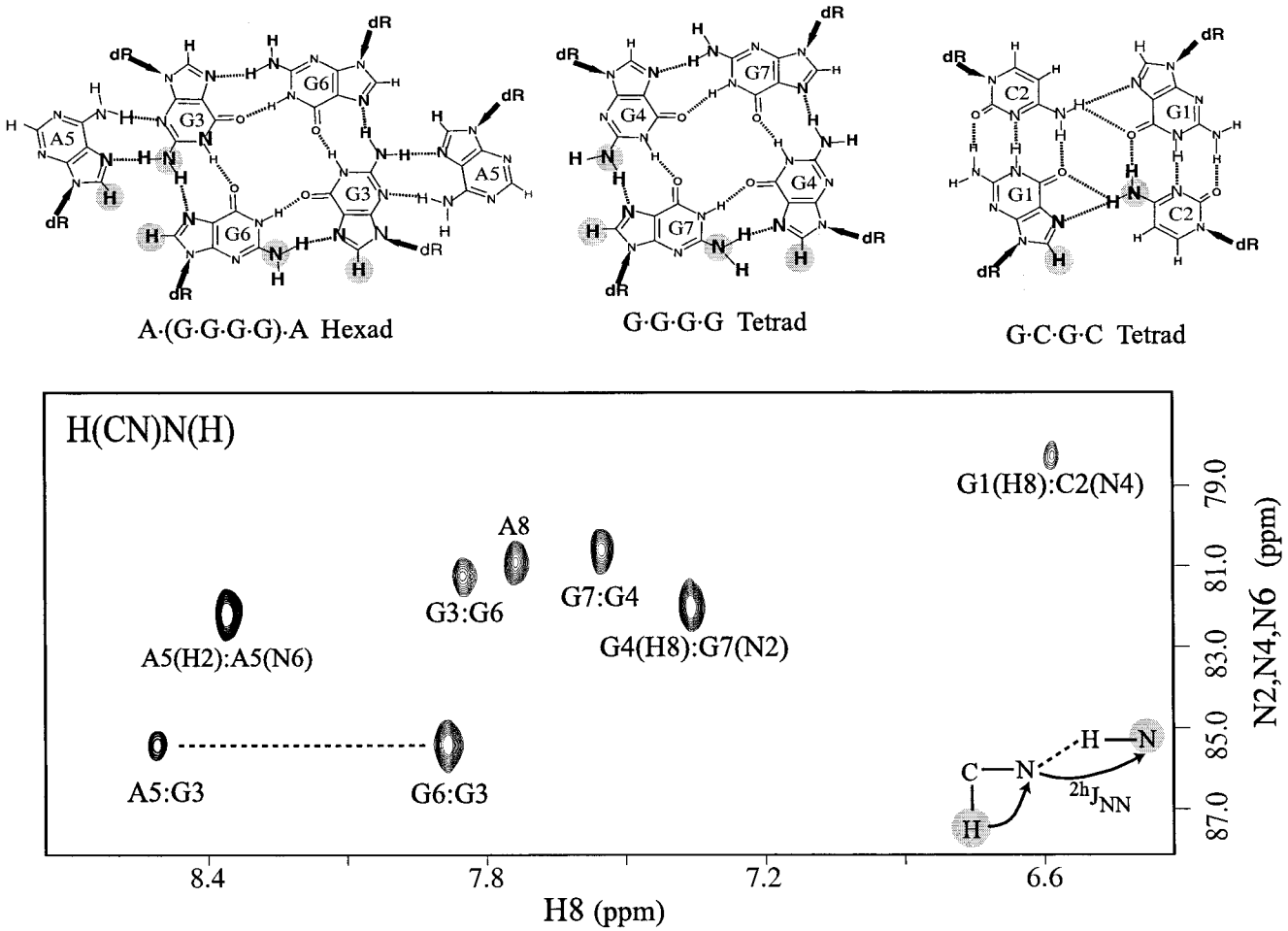

FIGURE 5. H(CN)N(H) spectrum of the hexad system (20 °C) showing H8(G,ω_2):N2(G,ω_1), H8(G,ω_2):N4(C,ω_1), and H8(A,ω_2):N2(G,ω_1) cross peaks to identify NH2···N7 hydrogen bonds within the tetrad and hexad motifs (shown above with the correlated nuclei indicated with gray circles) in the absence of detectable amino protons. The magnetization transfer pathway is indicated at bottom right. Two intranucleotide cross peaks, H2(A5/A8,ω_2):N6(A5/A8,ω_1), are also observed.

differ only in magnetization transfer pathways. In both spectra, the H2 proton of A7 shows an H2(A7,ω_2):N6(A7,ω_1) auto peak to the intraresidue amino N6 nitrogen, and a H2(A7,ω_2):N3(G3,ω_1) cross peak to the N3 nitrogen of G3, mediated via the $^{2h}J_{N6N3}$ coupling constant.

These sequences were then applied to the hexad system. Figure 6e shows an H2N6N3 spectrum in which the (A5)N6H$_2$···N3(G3) connectivity is established through an internucleotide (A5)H2:N3(G3) cross peak, in addition to an intranucleotide (A5)H2:N6(A5) auto peak. On the other hand, the H2 proton of A8, which is not involved in sheared G·A base pairing, shows only the (A8)H2:N6(A8) auto peak. The H2N6N3 and (H6)N6N3H2 sequences thereby act as useful companion techniques to the H(CN)N(H) sequence under exchange-broadening conditions. It must be noted that the H2N6N3 and (H6)N6N3H2 sequences require the sample to be $^{13}C/^{15}N$-labeled, whereas the H(CN)N(H) experiment may be performed on ^{15}N-labeled samples alone. In that sense, the H(CN)N(H) sequence should be more appropriately called H(N)N and the H2N6N3 and (H6)N6N3H2 sequences, H2(C6)N6N3 and (H6)N6(C6)N3H2, respectively.

Since N−H$_2$···N hydrogen bonds are ubiquitous in higher-order DNA structures, our efforts have largely focused on hydrogen bonds involving exchange-broadened amino protons. The groups of Williamson[34] and Marino[35] have independently reported elegant applications of the same principle for detecting structural and dynamical aspects of hydrogen bonds in RNA in the absence of detectable imino protons.

$^1H-^1H$ Correlations across Hydrogen Bonds. One of the inherent problems of $^{2h}J_{NN}$-COSY experiments is that the receptor nitrogen needs to be assigned in order to unambiguously identify the hydrogen bond. For many situations, this is a nontrivial task that is further complicated by the generally poor dispersion of (N_a,N_d) resonances. We recently addressed these problems by developing pulse sequences to obtain direct, inter-nucleotide correlations between protons in uniformly $^{13}C/^{15}N$-labeled nucleic acids containing $N_d-H\cdots N_a$ hydrogen bonds.[50,51] These sequences correlate H5(C) with H1(G) protons in G−C Watson−Crick, H2(A) with H3(T/U) protons in A-(T/U) Watson−Crick and H8(G/A) with exchangeable protons in various G·G and G·A mismatch base pairs. Under nonexchange broadening conditions, these ^1H-^1H connectivities circumvent the need for independent assignment of the donor/acceptor nitrogen and related degeneracy issues associated with the poorly dispersed nitrogen

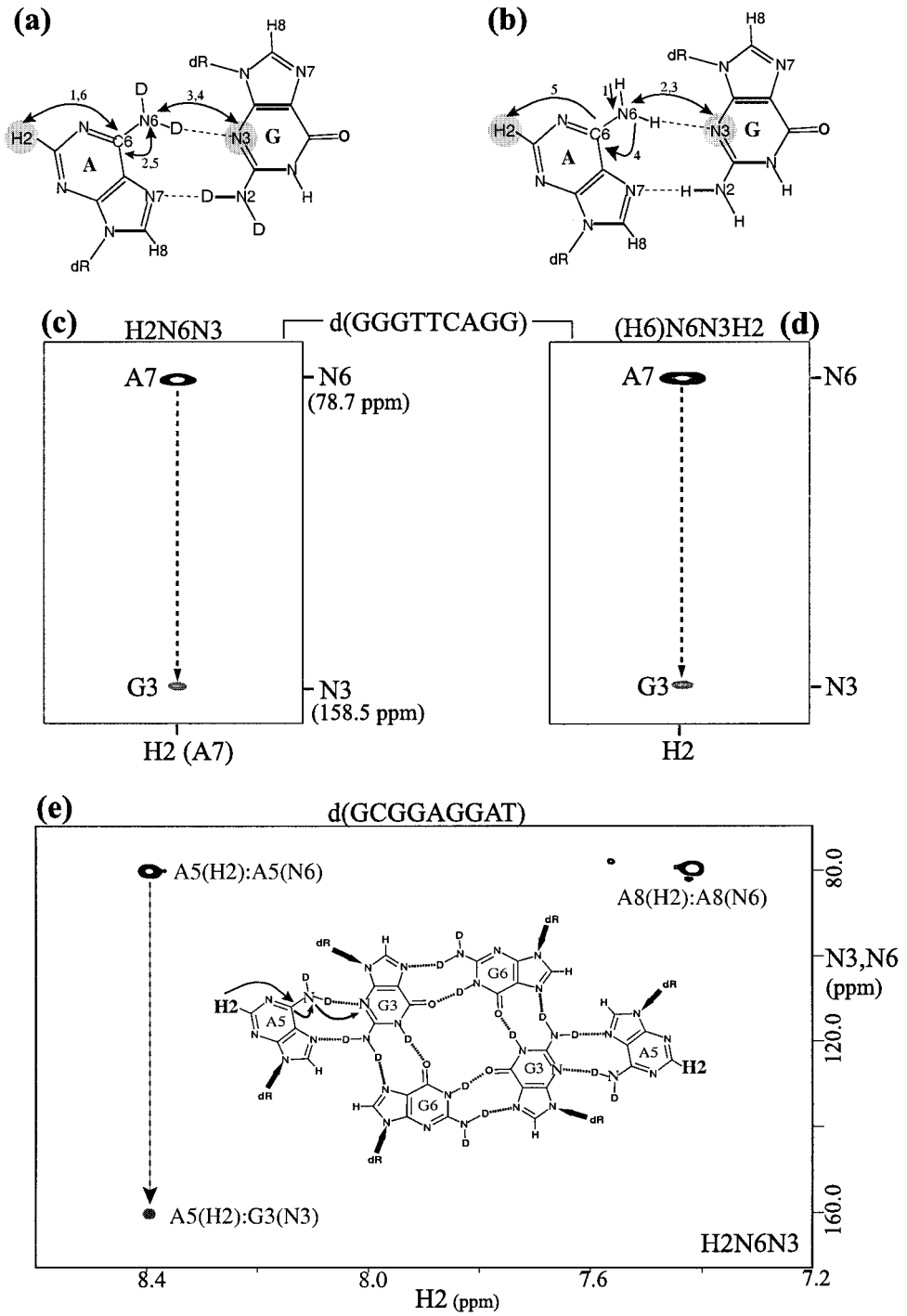

FIGURE 6. Spectra for identifying (A)N6H$_2$···N3(G) hydrogen bonds in sheared G·A mismatch alignments using the nonexchangeable H2 proton of adenine for detection. (a,b) Magnetization transfer pathways involved in the H2N6N3 and (H6)N6N3H2 sequences,[37] respectively. (c,d) Corresponding spectra recorded on the triad system (20 °C) showing H2(A7,ω_2):N6(A7,ω_1) auto- and H2(A7,ω_2):N3(G3,ω_1) cross peaks. (e) H2N6N3 spectrum of the hexad system (20 °C) showing H2(A5,ω_2):N6(A5,ω_1) auto- and H2(A5,ω_2):N3(G3,ω_1) cross peaks for complete identification of the hexad moiety.

resonances. Here, we illustrate application of these techniques to NH$_2$···N7 hydrogen bonds in G·G and sheared G·A mismatches.

The H(NN)H Experiment. Complete identification of NH$_2$···N7 hydrogen bonds from a soft HNN-COSY experiment is not possible until the N7 resonances are assigned independently, usually via H8−N7 correlations. Unfortunately, the dispersion of N7 nitrogens is usually poor, resulting in considerable degeneracy problems in the ^{15}N dimension. For example, it can be seen from Figure 4b that the N7 nitrogens of G1 and A7 are nearly degenerate, even in a relatively small system, such as the triad. In larger systems, this situation is likely to be further aggravated. To remedy this problem, we have developed an H(NN)H class of experiments which, under nonexchange broadening conditions, directly correlates (G/A/C) amino

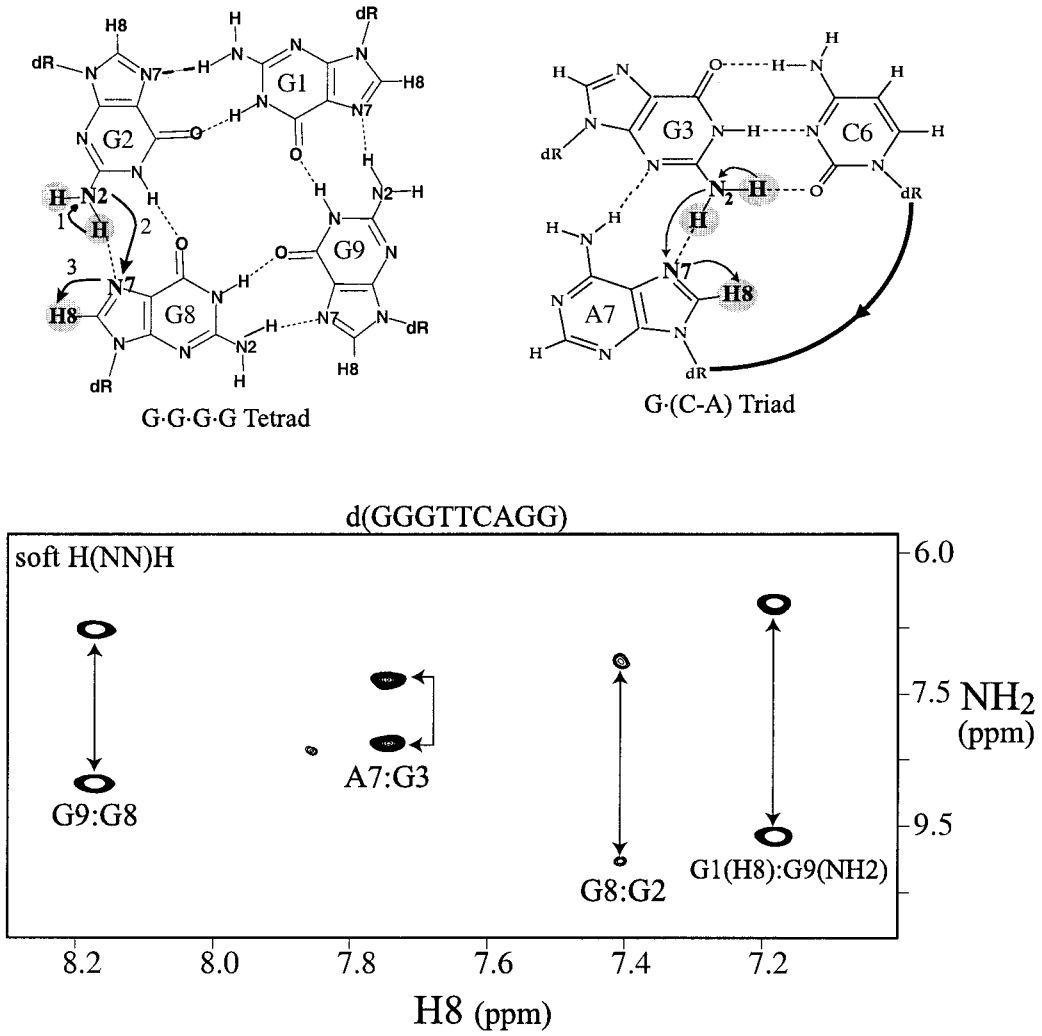

FIGURE 7. Soft H(NN)H spectrum of the triad system (0 °C) to demonstrate H8(ω_2):NH_2(ω_1) correlations across NH2···N7 hydrogen bonds via $^{2h}J_{N2N7}$ couplings. The magnetization transfer pathway is indicated schematically for the triad and tetrad motifs. The spectrum shows H8(A7,ω_2):$N2H_2$(G,ω_1) cross peaks to identify the (G3)$N2H_2$···N7(A7) linkage in the G3·(C6−A7) triad, three H8(G*p*,ω_2):$N2H_2$(Gq,ω_1) cross peaks to identify G·G connectivities in the tetrad. H8(p,ω_2):$N2H_2$(q,ω_1) cross peaks are labeled p:q.

protons with the H8 proton on the acceptor base across NH_2···N7−C8−H8 hydrogen bonds via the magnetization transfer pathway $H_2(t_1)$→N2(G)→N7(A/G)→H8(t_2). Figure 7 shows the soft H(NN)H spectrum of the triad system, consisting of H8(A/G,ω_2):$N2H_2$(G,ω_1) cross peaks within the triad and tetrad moeities. All of the NH_2(ω_2):N7(ω_1) correlations observed in the soft-HNN-COSY spectrum (Figure 4b) are present as equivalent H8(ω_2):NH_2(ω_1) connectivities in the soft H(NN)H spectrum. In addition, because detection utilizes nonexchangeable H8 protons, the H(NN)H spectrum shows additional H8(G8,ω_2):$N2H_2$(G2,ω_1) cross peaks that are missing from the soft HNN-COSY spectrum due to exchange-broadening of the G2 $N2H_2$ protons. Only the G1 $N2H_2$ protons remain too severely exchange-broadened to yield H8(G2):$N2H_2$(G1) cross peaks.

Since amino protons are rather susceptible to exchange broadening effects, it might appear that these experiments are of limited utility; however, even for a subset of the total number of hydrogen-bonded amino protons, $^1H-^1H$ correlations are always useful. Moreover, $^1H-^1H$ correlated experiments are not restricted to amino protons alone. The H(NN)H experiments may be applied to $N_d-H_d\cdots N_a-C-H_a$ hydrogen bonds involving imino protons as well, typical examples being (U/T)N3−H3···N1(A) Watson−Crick, (G)N1−H1···N1(A), and (G)N1−H1···N7(A/G) mismatches in which one can obtain similar $^1H-^1H$ connectivities through H2(A):H3(U/T), H2(A):H1(G), and H8(G/A):H1(G) correlations, respectively.[51]

Summary

We have attempted to highlight the tremendous impact of $^{2h}J_{NN}$ spectroscopy in the study of higher-order DNA structures, in terms of providing direct evidence for the hydrogen-bonded networks that bind the structural elements of these molecules. In this context, we have presented progress in NMR methodology that has simultaneously been developed in our laboratory to address the challenges presented by the diversity of hydrogen bonding alignments in different structural motifs. Although the sequences were demonstrated largely in the context of

G−C Watson−Crick base pairs and G·G and sheared G·A mismatches, they are generally applicable to all N−H···N hydrogen bonds. The molecular weights of the multistranded DNA systems presented here range from 6 to 10 kD. Although the pulse sequences described here are fairly sensitive for these systems, larger molecules will require considerably improved techniques, likely based on developments such as the availability of cryogenic probe technology at higher magnetic fields, in conjunction with TROSY[52]-based NMR methodology. It is quite conceivable that with the several-fold increase in sensitivity accompanying these developments, the tremendous benefits of $^{2h}J_{NN}$ coupling constants as well as those of the smaller interactions such as $^{4h}J_{NN}$ and $^{3h}J_{NC}$ may be extended to much larger systems soon.

We thank Dr. Abdelali Kettani for his significant contributions toward NMR studies of unusual DNA architectures and many useful discussions, Dr. Mateus Webba da Silva for structure determination of the hexad system, Dr. Aizhuo Liu for NMR methodology development, and Dr. Eugene Skripkin and Natalya Chernichenko for preparation of uniformly ^{13}C,^{15}N-labeled DNA oligomers. This research was supported by NIH GM-34504 to D.J.P.

References

(1) *DNA Structure and Recognition*; Neidle, S. Ed.; Oxford University Press: Oxford, 1994.

(2) Patel, D. J.; Bouaziz, S.; Kettani, A.; Wang, Y. Structures of Guanine-rich and Cytosine-rich Quadruplexes Formed in vitro by Telomeric, Centromeric and Triplet Repeat Disease Sequences. *Oxford Handbook of Nucleic Acid Structure*; Neidle, S., Ed.; Oxford University Press: Oxford, 1999; pp 389−453.

(3) Williamson, J. R. G-Quartet Structures in Telomeric DNA. *Annu. Rev. Biophys. Biomol. Struct.* **1994**, *23*, 703−730.

(4) Rhodes, D.; Giraldo, R. Telomere Structure and Function. *Curr. Opin. Struct. Biol.* **1995**, *5*, 311−312.

(5) Feigon, J.; Koshlap, K. M.; Smith, F. W. ^{1}H NMR Spectroscopy of DNA Triplexes and Quadruplexes. In *Methods in Enzymology*; James, T. Ed.; 1995; Vol. 261, pp 225−255.

(6) Sen, D.; Gilbert, W. The Structure of Telomeric DNA: DNA Quadruplex Formation. *Curr. Opin. Struct. Biol.* **1991**, *1*, 435−438.

(7) Arthanari, H.; Bolton, P. Functional and Dysfunctional Roles of Quadruplex DNA in Cells. *Chem. Biol.* **2001**, *8*, 221−230.

(8) Dingley, A. J.; Grzesiek, S. Direct Observation of Hydrogen Bonds in Nucleic Acid Base Pairs by Internucleotide $^2J_{NN}$ Couplings. *J. Am. Chem. Soc.* **1998**, *120*, 8293−8297.

(9) Pervushin, K.; Ono, A.; Fernandez, A.; Szyperski, T.; Kainosho, M.; Wüthrich, K. NMR Scalar Couplings across Watson−Crick Base Pair Hydrogen Bonds in DNA Observed by Transverse Relaxation-Optimized Spectroscopy. *Proc. Natl. Acad. Sci. U.S.A.*. **1998**, *95*, 14147−14151.

(10) Blake, P. R.; Lee, B.; Summers, M. F.; Adams, M. W.; Park, J.-B.; Zhou, Z. H.; Bax, A. Quantitative Measurement of Small Through Hydrogen-Bond and 'Through-Space' ^{1}H−^{113}Cd and ^{1}H−^{199}Hg J Couplings in Metal-substituted Rubredoxin from *Pyrococcus furiosus*. *J. Biomol. NMR* **1992**, *2*, 527−533.

(11) Blake, P. R.; Park, J.-B.; Adams, M. W.; Summers, M. F. Novel Observation of N−H···S(Cys) Hydrogen-Bond Mediated Scalar Coupling in ^{113}Cd−Substituted Rubredoxin from *Pyrococcus furiosus*. *J. Am. Chem. Soc.* **1992**, *114*, 4931−4933.

(12) Shenderovich I. G.; Smirnov S. N.; Denisov G. S.; Gindin V. A.; Golubev N. S.; Dunger A.; Reibke R.; Kirpekar S.; Malkina O. L.; Limbach H. H. Nuclear magnetic resonance of hydrogen bonded clusters between F^- and $(HF)_n$: Experiment and theory. *Ber. Bunsen Phys. Chem.* **1998**, *102*, 422−428.

(13) Dingley, A. J.; Cordier, F.; Grzesiek, S. An Introduction to Hydrogen Bond Scalar Couplings. *Concepts Magn. Reson.* **2001**, *13*, 103−127.

(14) Grzesiek, S.; Cordier, F.; Dingley, A. J. Scalar Couplings Across Hydrogen Bonds. *Methods. Enzymol.* **2001**, *338*, 111−133.

(15) Zidek L.; Stefl R.; Sklenar V. NMR methodology for the study of nucleic acids. *Curr. Opin. Struct. Biol.* **2001**, *11*, 275−281.

(16) Gemmecker, G. Direct Detection of Hydrogen Bonds in Biopolymers by NMR Spectroscopy. *Angew. Chem., Int. Ed. Engl.* **2000**, *39*, 1224−1226.

(17) Dingley, A. J.; Masse, J. E.; Peterson, R. D.; Barfield, M.; Feigon, J.; Grzesiek, S. Internucleotide Scalar Couplings Across Hydrogen Bonds in Watson−Crick and Hoogsteen Base Pairs of a DNA Triplex. *J. Am. Chem. Soc.* **1999**, *121*, 6019−6027.

(18) Liu, A.; Majumdar, A.; Hu, W.; Kettani, A.; Skripkin E.; Patel, D. J. NMR Detection of N−H···O═C Hydrogen Bonds in ^{13}C/^{15}N-Labeled Nucleic Acids. *J. Am. Chem. Soc.* **2000**, *122*, 3206−3210.

(19) Dingley, A. J.; Masse, J. E.; Feigon, J.; Grzesiek, S. Characterization of the Hydrogen Bond Network in Guanosine Quartets by Internucleotide $^{3h}J_{NC'}$ and $^{2h}J_{NN}$ Couplings. *J. Biomol. NMR* **2000**, *16*, 279−289.

(20) Liu, A.; Majumdar, A.; Jiang, F.; Chernichenko, N.; Skripkin, E.; Patel, D. J. NMR Detection of Intermolecular N−H···N Hydrogen Bonds in the Human T Cell Leukemia Virus-1 Rex Peptide-RNA Aptamer Complex; *J. Am. Chem. Soc.* **2000**, *122*, 11226-1127.

(21) Mishima, M.; Hatanaka, M.; Shigeyuki, Y.; Ikegami, T.; Wälchli, M.; Ito, Y.; Shirakawa, M. Intermolecular ^{31}P-^{15}N and ^{31}P-^{1}H Scalar Couplings Across Hydrogen Bonds Formed between a Protein and a Nucleotide *J. Am. Chem. Soc.* **2000**, *122*, 5883−5884.

(22) Löhr, F.; Mayhew, S. G.; Rüterjans, H. Detection of Scalar Couplings Across NH···OP and OH····OP Hydrogen Bonds in a Flavoprotein. *J. Am. Chem. Soc.* **2000**, *122*, 9289−9295.

(23) Wöhnert, J.; Dingley, A. J.; Stoldt, M.; Gorlach, M.; Grzesiek, S.; Brown, L. R. Direct identification of NH···N hydrogen bonds in noncanonical base pairs of RNA by NMR spectroscopy. *Nucleic Acids Res.* **1999**, *27*, 3104−3110.

(24) Kettani, A.; Bouaziz, S.; Skripkin, E.; Majumdar, A.; Wang, W.; Jones, R. A.; Patel, D. J. Interlocked Mismatch-aligned Arrowhead DNA Motif. *Structure*, **1999**, *7*, 803−815.

(25) Kettani, A.; Gorin, A.; Majumdar, A.; Hermann, T.; Skripkin, E.; Zhao, H.; Jones, R. A Dimeric DNA Interface Stabilized by Stacked A·(G·G·G·G)·A Hexads and Bound Monovalent Cation. *J. Mol. Biol.* **2000**, *297*, 627−644.

(26) Kettani, A.; Basu, G.; Gorin, A.; Majumdar, A.; Skripkin, E.; Patel, D. J. A Template Based Approach to G·(C−A) Base Triad Formation: Implications for DNA Architecture of (CAG)n Triplet Repeat. *J. Mol. Biol.* **2000**, *301*, 129−146.

(27) Jiang, L.; Majumdar, A.; Hu, W.; Jaishree, T. J.; Xu, W.; Patel, D. J. Saccharide-RNA Recognition in a Complex Formed between Neomycin B and an RNA Aptamer. *Structure* **1999**, *7*, 817−827.

(28) Al-Hashimi, H. M.; Majumdar, A.; Gorin, A.; Kettani, A.; Skripkin, E.; Patel, D. J. Field- and Phage-Induced Dipolar Couplings in a Homodimeric DNA Quadruplex: Relative Orientation of G·(C−A) Triad and G-Tetrad Motifs and Direct Determination of C2 Symmetry Axis Orientation. *J. Am. Chem. Soc.* **2001**, *123*, 633−640.

(29) Al-Hashimi, H. M.; Gorin, A.; Majumdar, A.; Patel, D. J. Alignment of the HTLV−I Rex Peptide Bound to Its Target RNA Aptamer from Magnetic Field-Induced Residual Dipolar Couplings and Intermolecular Hydrogen Bond. *J. Am. Chem. Soc.* **2001**, *123*, 3179−3180.

(30) Gosser, Y.; Hermann, T.; Majumdar, A.; Hu, W.; Frederick, R.; Jiang, F.; Xu W.; Patel, D. J. Peptide-triggered conformational switch in HIV-1 RRE RNA complex. *Nat. Struct. Biol.* **2001**, *8*, 146−150.

(31) Majumdar, A.; Kettani, A.; Skripkin, E. Observation and Measurement of Internucleotide $^2J_{NN}$ Coupling Constants between ^{15}N Nuclei with Widely Separated Chemical Shifts. *J. Biomol. NMR*. **1999**, *14*, 67−70.

(32) Hennig, M.; Geierstanger, B. H. Direct Detection of a Histidine−Histidine Side Chain Hydrogen Bond Important for Folding of Apomyoglobin. *J. Am. Chem. Soc.* **1999**, *121*, 5123−5126.

(33) Majumdar, A.; Kettani, A.; Skripkin, E.; Patel, D. J. Observation of Internucleotide NH···N Hydrogen Bonds in the Absence of Directly Detectable Proton. *J. Biomol. NMR*. **1999**, *15*, 207−211.

(34) Hennig, M.; Williamson, J. R. Detection of NH···N Hydrogen Bonding in RNA via Scalar Couplings in the Absence of Observable Imino Proton Resonances. *Nucleic Acids Res.* **2000**, *28*, 1585−1593.

(35) Luy, B.; Marino, J. Direct Evidence for Watson−Crick Base Pairs in a Dynamic Region of RNA Structure. *J. Am. Chem. Soc.* **2000**, *122*, 8095−8096.

(36) Kojima, C.; Ono, A.; Kainosho, M. Studies of physicochemical properties of N−H···N hydrogen bonds in DNA, using selective ^{15}N-labeling and direct ^{15}N 1D NMR. *J. Biomol. NMR*. **2000**, *18*, 269−277.

(37) Majumdar, A.; Kettani, A.; Skripkin, E.; Patel, D. J. Pulse Sequences for Detection of NH_2···N Hydrogen Bonds in Sheared G·A Mismatches via Remote, non-Exchangeable Protons. *J. Biomol. NMR* **2001**, *19*, 103−113.

(38) Pervushin, K. V.; Fernandez, C.; Riek, R.; Ono, A.; Kainosho, M.; Wüthrich, K. Determination of $^{h2}J_{NN}$ and $^{h1}J_{HN}$ coupling constants across Watson−Crick base pairs in the Antennapedia homeodomain−DNA complex using TROSY. *J. Biomol. NMR*. **1998**, *12*, 345−348.

(39) Golubev, N. S.; Shenderovich, I. G.; Smirnov, S. N.; Denisov, G. S.; Limbach, H. H. Nuclear Scalar Spin−Spin Coupling Reveals Novel Properties of Low-Barrier Hydrogen Bonds in a Polar Environment. *Chem. Eur. J.* **1999**, *5*, 492−497.
(40) Yan, X. Z.; Kong, X. M.; Xia, Y. L.; Sze, K. H.; Zhu, G. Determination of Internucleotide $^{1h}J_{HN}$ Couplings by the Modified 2D J_{NN}-Correlated [^{15}N, ^{1}H] TROSY. *J. Magn. Reson.* **2000**, *147*, 357−360.
(41) Wu, Z.; Ono, A.; Kainosho, M.; Bax, A. H···N hydrogen bond lengths in double stranded DNA from internucleotide dipolar couplings *J. Biomol. NMR* **2001**, *19*, 361−365.
(42) Pervushin, K. The use of TROSY for detection and suppression of conformational exchange NMR line broadening in biological molecules *J. Biomol. NMR* **2001**, *20*, 275−285.
(43) Scheurer, C.; Brüschweiler, R. Quantum-chemical characterization of nuclear spin−spin couplings across hydrogen bonds. *J. Am. Chem. Soc.* **1999**, *121,* 8661−8662.
(44) Benedict H.; Shenderovich, I. G.; Malkina, O. L.; Malkin, V. G.; Denisov, G. S.; Golubev, N. S.; Limbach, H. H. Nuclear Scalar Spin−Spin Couplings and Geometries of Hydrogen Bonds. *J. Am. Chem. Soc.* **2000**, *122,* 1979−1988.
(45) Barfield, M.; Dingley, A. J.; Feigon, J.; Grzesiek, S. A DFT study of the interresidue dependencies of scalar *J*-coupling and magnetic shielding in the hydrogen-bonding regions of a DNA triplex. *J. Am. Chem. Soc.* **2001**, *123,* 4014−4022.
(46) Bryce, D. L.; Wasylishen, R. E. Modeling $^{2h}J_{iso}$(N, N) in nucleic acid base pairs: Ab initio characterization of the ^{2h}J(N, N) tensor in the methyleneimine dimer as a function of hydrogen bond geometry, *J. Biomol. NMR* **2001**, *19*, 371−375.
(47) Zhang, N.; Gorin, A.; Majumdar, A.; Kettani, A.; Chernichenko, N.; Skripkin E.; Patel, D. J. An A·(G·G·G·G) pentad-containing dimeric DNA quadruplex defined by double chain reversal, edgewise and V-shaped turns linking stacked G(anti)·G(anti)·G(anti)·G(syn) tetrads. *J. Mol. Biol.* **2001**, *311*, 1063−1079.
(48) ^{13}C/^{15}N-labeled DNA samples were synthesized enzymatically using a modification of the Zimmer and Crothers[24,49] procedure. NMR samples were prepared in H_2O or D_2O buffer (100−150 mM NaCl, 2 mM phosphate at pH 6.6) at concentrations of 1−1.5 mM. All spectra were recorded on 600 MHz Varian INOVA spectrometers. All spectra (Figures 3−7) were acquired in <5h.
(49) Zimmer, D. P.; Crothers, D. M. NMR of Enzymatically Synthesized Uniformly ^{13}C,^{15}N-Labeled DNA Oligonucleotides. *Proc. Natl. Acad. Sci. U.S.A.* **1995**, *92*, 3091−3095.
(50) Majumdar, A.; Gosser, Y.; Patel, D. J. ^{1}H-^{1}H Correlations Across N−H···N Hydrogen Bonds in Nucleic Acids. *J. Biomol. NMR* **2001**, *21*, 289−306.
(51) Majumdar, A. Applications of $^{1}H_a$_$^{1}H_d$ Correlated $^{2h}J_{NN}$ Spectroscopy for Identifying $H_a-C-N_a\cdots H_d-N_d$ Hydrogen Bonds in Nucleic Acids. *Magn. Reson. Chem.* **2001**, *39*, 5166−5170.
(52) Pervushin, K.; Riek, R.; Wider, G.; Wüthrich, K. Attenuated T2 relaxation by mutual cancellation of dipole−dipole coupling and chemical shift anisotropy indicates an avenue to NMR structures of very large biological macromolecules in solution. *Proc. Natl. Acad. Sci. U.S.A.* **1997**, *94*, 12366−12371.
(53) Karsten, T.; Dingley, A. J.; Hoffmann, A.; Omichinski, J. G.; Grzesiek, S.; Determination of backbone nitrogen−nitrogen J correlations in proteins *J. Biomol. NMR*, **1997**, *10*, 403−408.
(54) Löhr, F.; Rüterjans, H. Detection of Nitrogen−Nitrogen J-Couplings in Proteins *J. Magn. Reson.* **1998**, *132*, 130−137.

AR010097+